Polymer Chemistry

RSC Publishing

PAPER

View Article Online
View Journal | View Issue

Cite this: *Polym. Chem.*, 2013, **4**, 2489

Template synthesis of PMAA@chitosan hollow nanorods for docetaxel delivery

Yajuan Sun,[a] Weibing Dong,[bc] Huiyuan Wang,[d] Yongzhuo Huang,*[d] Huike Gu,[a] Victor C. Yang*[ef] and Junbo Gong*[ab]

Received 30th December 2012
Accepted 4th February 2013

DOI: 10.1039/c3py21157f

www.rsc.org/polymers

Nanorods are capable of enhanced intracellular delivery and prolonged blood circulation over their spherical counterparts, and thus can be used as unmatched drug carriers for cancer chemotherapy. An innovative method was developed to synthesize size-tunable, PMAA@chitosan-based, hollow polymeric nanorods for intracellular delivery, by using mesoporous silica nanorod templates. The morphology of the polymeric hollow nanorods was examined by TEM and FT-IR spectra, which indicated a homogeneous three-dimensional structure. An uptake study using human lung carcinoma A-549 cell lines revealed highly efficient cell internalization of the FITC-labeled nanorods, suggesting the potential of utilizing these nanorods as carriers in achieving effective intracellular drug delivery. Cell viability studies of the docetaxel-loaded nanorods yielded consistent results, as the drug-loaded nanorods produced a significantly higher inhibition of the growth of A-549 tumor cells when compared with treatment by free docetaxel. Overall, this preliminary *in vitro* investigation sheds light on the use of prepared hollow polymeric nanorods for drug delivery applications.

Introduction

Nanorods have received considerable attention due to their promising applications in diagnosis,[1] imaging,[2] and drug delivery.[3] Their uniquely large surface area-to-volume ratio enables nanorods to carry a large payload.[3,4] More attractively, recent research has demonstrated that one-dimensional rod-shaped carriers have advantages over their spherical counterparts in both blood circulation time and cell internalization rates.[5–7] The shape-related effects and their benefits for improving *in vivo* profiles have been investigated in drug delivery and bio-imaging. For instance, DNA-modified gold nanorods were used for gene delivery[3,8] and high-contrast paramagnetic fluorescent mesoporous silica nanorods were produced as multifunctional cell-imaging probes.[9]

However, current studies mainly focus on inorganic nanorods, such as noble metal nanorods[10] and silica nanorods.[11] A major drawback of inorganic materials is their poor biodegradability and biocompatibility.[12] Recent studies show that mesoporous silica nanoparticles with diameters ranging from 150 nm to 4 μm induced substantial cytotoxicity at high concentrations *in vitro*, and caused severe systemic toxicity *in vivo* after intra-peritoneal and intra-venous injections.[13] Another challenge for their application as drug carriers is the low drug-loading efficiency, because the drug-loading process relies on either chemical conjugation or physical adsorption to the surface of the metal nanorods. For instance, the amount of doxorubicin incorporated onto the gold nanorods was reported to be a mere 0.84 wt%.[14] More critically, water-insoluble drugs are often incompatible to these loading processes.[15,16] To overcome these problems, we developed a hollow polymeric nanorod for the purpose of drug delivery based on a novel template synthesis strategy.

Polymeric drug delivery systems have been widely used in cancer therapy due to their multi-functionality, biodegradability and great variation in the physical/chemical properties. Polymers contain a variety of functional groups, and thus proper tailoring can aid in the design of polymers possessing varying physicochemical properties that are suitable for the delivery of a broad spectrum of different drugs.[17] Indeed, recent advances in drug delivery research have enabled the rational design of polymer carriers with desirable biological functions that are tailored for the delivery of specific drug cargos.[18] Poly(methacrylic acid) (PMAA) microcapsules have been prepared

[a]*State Key Laboratory of Chemical Engineering, School of Chemical Engineering and Technology, Tianjin University, Tianjin 300072, China. E-mail: junbo_gong@tju.edu.cn*

[b]*Tianjin Key Laboratory of Modern Drug Delivery & High-Efficiency, School of Pharmacy, Tianjin University, Tianjin 300072, China*

[c]*Department of Chemistry, School of Science, Tianjin University, Tianjin 300072, China*

[d]*Shanghai Institute of Materia Medica, Chinese Academy of Sciences, Shanghai 201203, China. E-mail: yzhuang@simm.ac.cn*

[e]*Tianjin Key Laboratory on Technologies Enabling Development of Clinical Therapeutics and Diagnosis, School of Pharmacy, Tianjin Medical University, Tianjin 300070, China*

[f]*College of Pharmacy, University of Michigan, Ann Arbor, Michigan, USA. E-mail: vcyang@umich.edu*

for the controlled release of doxorubicin based on its specific pH-sensitive properties.[19,20] In addition, chitosan (CS) has been employed to assemble into microspheres for protein drug delivery, owing to its biodegradable, nontoxic and biocompatible characteristics.[21,22]

Mesoporous silica (SiO_2) particles with a high surface area, controllable pore size and pore structure, and tunable size and morphology appear to be excellent template materials for the preparation of drug-containing vehicles.[23–25] High drug-loading efficiency can be achieved by using the mesoporous silica microsphere as a synthesis template and applying the layer-by-layer (LBL) technique in fabricating spherical polymeric particles.[13,26] Motivated by this principle, herein we developed a novel template synthesis strategy based on the use of mesoporous silica nanorods for the construction of hollow polymeric nanorods with double walls (Scheme 1). The pH-sensitive PMAA and highly biocompatible chitosan were employed to construct the inner and outer polymeric shells, respectively. To demonstrate the drug delivery capacity of these nanorod vehicles, docetaxel was selected as the model drug due to its widely accepted clinical use in treating breast, ovarian, prostate, and non-small cell lung cancers.[27,28] The hybrid cross-linked polymer-coated silica nanorods were synthesized by encapsulation of the nanorods *via* distillation precipitation polymerization, sol–gel processing, and cross-linking polymerization. After the silica templates were etched with hydrofluoric acid, the final PMAA@CS hollow nanorods were successfully obtained. Characterization of these nanorod carriers was conducted by TEM, Fourier transform infrared spectroscopy, and thermogravimetric analysis. Furthermore, the antitumor potential of the docetaxel-loaded nanorods was also examined and compared with free docetaxel using an A-549 cancer cell line culture.

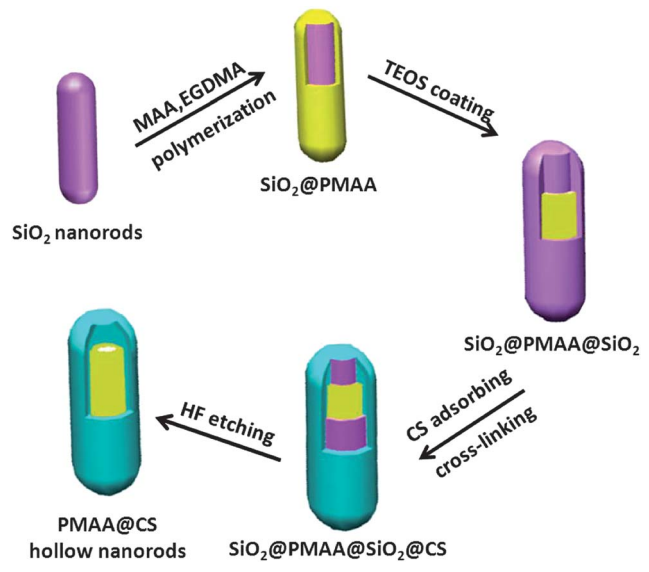

Scheme 1 Schematic illustration of the multi-layer hybrid nanorods and corresponding hollow polymeric nanorods.

Experimental

Chemicals

Cetyltrimethylammonium bromide (CTAB), 3-(trimethoxysilyl)-propylmethacrylate (MPS), methacrylic acid (MAA), ethylene glycol dimethacrylate (EGDMA), 2,2′-azobis(isobutyronitrile) (AIBN), butanedioic anhydride, 3-aminopropyl triethoxysilane (APTES) were obtained from Aladdin chemistry Co. (Shanghai, China). Tetraethyl orthosilicate (TEOS), aqueous ammonia, ethanol, acetonitrile, *N*,*N*-dimethylformamide (DMF), and hydrofluoric acid were purchased from Tianjin Kemiou Chemical Reagent Co. (Tianjin, China). CS (M_w = 200 kDa) was obtained from Beijing Biodee Biotechnology Co. (Beijing, China). Docetaxel (>98%) was purchased from Dalian Meilun Biotech Co. (Dalian, China). Unless otherwise stated, purified water with a resistivity of 18 MΩ cm was used in all experiments.

Synthesis of the silica/polymer multilayer hybrid nanorods

The synthesis of the mesoporous silica nanorods was conducted according to a well-established sol–gel process with a slight modification.[29] In brief, cetyltrimethylammonium bromide solution precursor was prepared by adding 1.6 mmol CTAB into 140 mL water mixed with 4.5 mL aqueous ammonia (28–30%) under magnetic stirring for 1 h at room temperature. To the mixed solution, 2.5 mL TEOS was then added. The reaction proceeded with vigorous stirring at 40 °C for 3 h. The resulting nanorods were washed several times with deionized water and ethanol. MPS-modified silica templates were prepared according to the Stöber method, by reacting 1.0 g silica nanorods with 0.5 mL MPS at 40 °C with vigorous stirring for 12 h.[30] Following the reaction, the resultant MPS-modified silica nanorods (SiO_2-MPS) were purified *via* five cycles of centrifugation and dispersion in ethanol and water. The SiO_2@PMAA hybrid nanorods were then prepared by distillation precipitation polymerization of methacrylic acid in acetonitrile with a cross-linker EGDMA, according to an established protocol.[19,31] Concisely, about 0.2 g of the SiO_2-MPS nanorods was dispersed into 80 mL acetonitrile under ultrasonication in a 100 mL flask, equipped with a fractionation column, a condenser, and a receiver. A mixture of MAA (0.82 mL, 0.01 mol), EGDMA (0.28 mL, 0.0015 mol) and 2,2′-azobis(isobutyronitrile) (AIBN, 0.02 g) was then introduced into the flask to initiate the polymerization process. The reaction was continued under reflux conditions and then stopped after approximately 1.5 h by distilling off 40 mL of the acetonitrile. The resulting SiO_2@PMAA hybrid nanorods were treated with five cycles of centrifugation and re-dispersion in acetonitrile and ethanol to remove the unreacted monomers and oligomers. Following the formation of the PMAA shell, a carboxylated silica layer was coated onto the surface of the SiO_2@PMAA nanorods, using a previously reported method.[19,32] After that, about 0.2 g SiO_2@PMAA hybrid nanorods and 3.0 mL ammonia were dispersed into a water–ethanol (20 mL/160 mL) mixture under ultrasonication, followed by dropwise addition of 1.0 mL TEOS into the flask with vigorous stirring at room temperature for 6 h. The resultant solution was treated with five cycles of centrifugation and dispersion in ethanol and water.

Then the obtained SiO_2@PMAA@SiO_2 nanorods were re-dispersed in 20 mL DMF. In a separate pot, a solution of 1.7 mmol butanedioic anhydride, 0.4 mL APTES and 50 mL DMF were stirred at room temperature for 3 h. To this solution, the previously prepared DMF solution of SiO_2@PMAA@SiO_2 and 2 mL deionized water were added, and the mixture was stirred for 5 h. The resultant solution was then purified by five centrifugation–dispersion cycles using water.

The final SiO_2@PMAA@SiO_2@CS tetra-layer hybrid nanorods were fabricated *via* the process of cross-linking polymerization, using glutaraldehyde (GA) as the cross-linker.[21] Briefly, 2 wt% chitosan (CS) solution was prepared by mixing 0.4 g of CS with 40 mL acetic acid. A solution containing 0.1 g of SiO_2@PMAA@SiO_2–COOH in 25 mL water was then added dropwise into the CS solution under stirring for 1 h, and the mixture was centrifuged at 2000 × *g* for 20 min. The precipitate was re-dispersed in water *via* sonication, and centrifuged again for 20 min. The dispersion–centrifugation cycle was repeated three times to remove any remaining CS. Lastly, the resulting particles were treated with glutaraldehyde (3.0 mL, 2.5%) for 5 h at 40 °C, and the final product was purified through three centrifugation–dispersion cycles, using water as the re-dispersion vehicle.

Fabrication of PMAA@CS hollow nanorods

The PMAA@CS hollow nanorods were prepared by removal of the silica layers from the SiO_2@PMAA@SiO_2@CS tetra-layer hybrid nanorods. In brief, the multilayer hybrid nanorods were stirred in 20% hydrofluoric acid (HF) for 4 h. The excess HF and SiF_4 were then extracted from the hollow nanorods by five cycles of centrifugation–dispersion in water. The etching process was repeated three times to completely remove the silica layers. Finally, the hollow nanorods were dialyzed in water for one week.

Characterization

Morphologies of the nanorods prepared in this work were examined on JEOL S-4800 field-emission scanning electron microscopes. TEM micrographs were obtained on a JEM-2100F transmission electron microscope, by placing the nanorods on a copper grid with a carbon membrane. Fourier transform infrared spectra were obtained on a Bruker TENSOR 27 FT-IR spectrometer over potassium bromide pellets and the diffuse reflectance spectra were scanned over the range 4000–400 cm^{-1}. The drug loading efficiency was measured using an Agilent technologies 1200 HPLC series equipped with an Agilent Eclipse XDB-C18 column. Fluorescence images were obtained from an Olympus IX70 microscope (Japan). Absorbance was measured using a Thermo F1 microplate reader. Thermogravimetric analysis (TGA) was performed with a SHIMADZU TGA-50 system at a heating rate of 10 °C min^{-1} to 700 °C in a N_2 atmosphere.

In *vitro* release studies

The release studies of docetaxel from the polymeric nanorods were performed by incubating a sample of the formulation with phosphate buffered solution (PBS, pH = 7.4) under sink conditions. The samples sealed in a dialysis bag (MWCO 6–8k) were placed in an incubator at 37 °C with horizontal shaking. 2 mL aliquots of supernatant solution were withdrawn at designated sampling intervals (4, 8, 12, 22, 26, 30, 34, 46, and 50 h) and replaced with the same amount of fresh buffer. The amount of released docetaxel was analyzed by HPLC. The experiments were performed in triplicate.

Fluorescence microscopy

A-549 cells were seeded at 5×10^5 cells per well in six-well plates and allowed to adhere for 24 h at 37 °C. The cells were washed twice with sterile PBS to remove non-adhered cells prior to treatment with FITC-labeled hollow nanorods (*ca.* 5 μg mL^{-1}). Cells at different populations were then incubated with FITC-labeled hollow nanorods in 1640 medium for 4 h at 37 °C, washed twice with PBS and then imaged using a fluorescence microscope.

MTT assay

Cell viability assays were performed in duplicate *via* mitochondrial reduction of 3-(4,5-dimethylthiazolyl-2)-2,5-diphenyltetrazolium bromide (MTT) to purple formazan.[33,34] Briefly, A-549 cells were grown in 1640 supplemented with 10% of fetal bovine serum (FBS) and maintained in a humidified incubator. 100 μL aliquots of concentration 6.0×10^5 cells per mL were placed into wells of a 96-well plate and incubated for 48 h. The wells were treated with different concentrations of PMAA@CS hollow nanorods and incubated for 48 h before 10 μL of MTT reagent was added to each well. After another 4 h incubation, 150 μL of DMSO was added to each well, and the ratiometric absorption measurements were then performed using an automated reader at 490 nm.

Results and discussion

The PMAA@CS hollow nanorods were successfully fabricated following the procedure illustrated in Scheme 1. First, mesoporous silica nanorods with different diameters and aspect ratios were synthesized by controlling the concentrations of aqueous ammonia and cetyltrimethyl ammonium bromide. As shown in Fig. 1, both the SEM (a and c) and TEM images (b and d) revealed the formation of calcined silica nanorods possessing well-defined shapes. The size of the nanorods is calculated to be 80 ± 17 nm in width, and 260 ± 25 nm in length based on statistics data in the TEM images. The surface area of the mesoporous silica nanorods, measured by nitrogen adsorption experiments, was found to be 945 m^2 g^{-1}, with an average pore size of 2.55 nm and a pore volume of 1.13 mL g^{-1} (see Fig. 1e).

PMAA was chosen as the inner shell material, primarily due to its stimuli-sensitive behavior. It is noted that PMAA would possess Donnan osmotic swelling properties, owing to the ionization of carboxylic acid groups at high pH. Hence, swelling of the PMAA would trigger the release of the drug from the core. On the other hand, lowering the pH would shrink the shell, rendering the drug to release at a lower level. Because of the pH-responsive behavior of the PMAA shell, one could easily

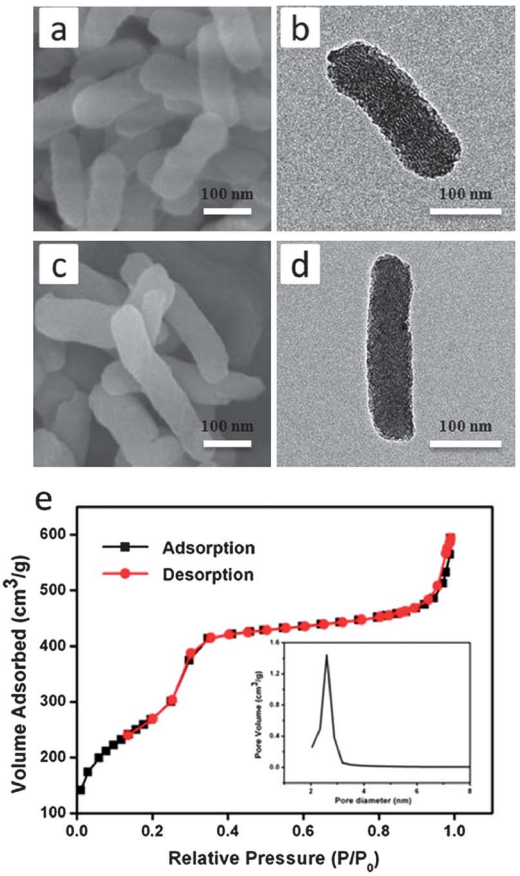

Fig. 1 SEM (a and c) and TEM (b and d) images of the mesoporous silica nanorods with different aspect ratios of 2.7 (a and b) and 4.0 (c and d). (e) Nitrogen sorption isotherm and BJH pore size distribution plots (inset) of mesoporous silica nanorods, calcined at 600 °C for 6 h. The desorption branch (red line) of the nitrogen isotherm is used to calculate the pore size.

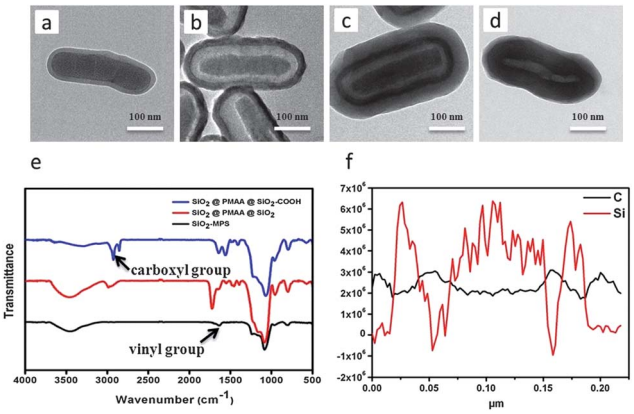

Fig. 2 TEM images of the (a) SiO_2@PMAA nanorods; (b) SiO_2@PMAA@SiO_2 nanorods; (c) SiO_2@PMAA@SiO_2@CS nanorods and (d) PMAA@CS hollow nanorods. (e) FT-IR spectra of SiO_2-MPS, SiO_2@PMAA@SiO_2 and SiO_2@PMAA@SiO_2–COOH. (f) Energy dispersive X-ray fluorescence spectra of SiO_2@PMAA@SiO_2@CS.

regulate the drug release rate by altering the pH of the environment.[19,32]

In order to facilitate the deposition and coating of PMAA on the nanorod surfaces, vinyl-functionalized nanorods (SiO_2-MPS) were synthesized. PMAA was coated on the surface of the SiO_2-MPS nanorods through the radical copolymerization of the monomer MAA and the cross-linker ethylene glycol dimethacrylate (EGDMA) in the presence of 2,2′-azobis(isobutyronitrile) (AIBN) as an initiator. An absorption peak at 1636 cm^{-1} (arrow in Fig. 2e) in the FT-IR spectrum of SiO_2-MPS was observed, indicating that the carbon–carbon double bonds were successfully grafted on the surface of the rod-like mesoporous silica. The TEM image (Fig. 2a) reveals that the SiO_2@PMAA possesses a smooth particle surface and an obvious contrast ratio, suggesting successful deposition of the PMAA layer on the surface of the mesoporous silica nanorods. Estimated from the TEM images, the average size of the polymer-coated nanorods appears to increase from 70 nm for the original non-coated particles to about 105 nm in diameter for SiO_2@PMAA. As is known, the thickness of the PMAA layer can be fine-tuned by adjusting the amount of monomer and the ratio between the monomer and cross-linker. Our result shows that as the amount of monomer increased from 0.50 mL to 1.20 mL, the thickness grew from 12 nm to 50 nm. However, when the thickness is greater than 35 nm, TEM analysis revealed that the formed nanorods exhibit a poor polydispersity. With this in mind, the balance between the concentrations of the cross-linker, monomer, initiator and the template should first be optimized, so that a desirable thickness of the coating can be attained.

Chitosan (CS) is well-recognized as a biocompatible coating material,[35] and is therefore an excellent candidate to improve both the surface properties and the toxicity of the developed hollow nanorods. Nevertheless, it was quickly discovered that direct deposition of chitosan on the outside layer of the nanorods could not be achieved, primarily due to its weak interaction with PMAA. To solve this problem, we developed a facile method by first depositing a carboxylated silica layer on the PMAA shell, and then using it as a template to support the coating of the CS layer. As displayed in Fig. 2b, a layer of silica was successfully coated on the outer surface of SiO_2@PMAA *via* a sol–gel process. FT-IR spectra of SiO_2@PMAA@SiO_2 and carboxyl-modified SiO_2@PMAA@SiO_2 clearly confirmed carboxylation of the outside silica layer (Fig. 2e). Chitosan was then adsorbed on the modified outer silica layer through electrostatic interactions between the carboxyl groups on silica and the amino groups on chitosan. This CS shell was further solidified by cross-linking using glutaraldehyde, prior to the removal of the silica template. Both the TEM image (Fig. 2c) and the energy dispersive X-ray fluorescence spectra (Fig. 2f) clearly demonstrated the successful deposition of the CS layer on the nanorods through cross-linking polymerization. It is worth noting that the thickness of the CS shell can be readily controlled, simply by altering the amount or molecular weight of CS. After the selective removal of SiO_2 with a HF solution, hollow polymeric nanorods with intact structures were obtained, as shown by the TEM image in Fig. 2d. The size of the polymeric nanorods is measured to be 118 ± 20 nm in width and 257 ± 24 nm in length based on statistics data in the TEM images.

Fig. 3 presents the TGA results of the prepared nanorods. As seen in Fig. 3, a trivial weight loss of 3.08% was observed

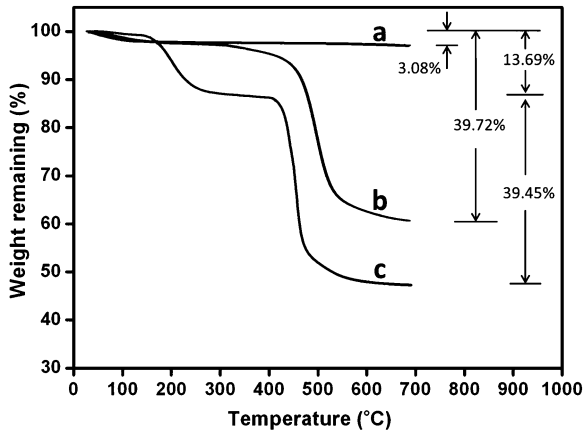

Fig. 3 Thermogravimetric analysis (TGA) results of (a) SiO_2, (b) SiO_2@PMAA and (c) SiO_2@PMAA@SiO_2@CS nanorods.

probably owing to thermal removal of the water absorbed onto the mesoporous silica. Alternatively, a sustained and significant weight loss of 39.72% was noted for SiO_2@PMAA, presumably attributed to the additional PMAA coating on the silica nanorods. In sharp contrast, a rapid weight loss of 13.69%, occurring at the melting point of chitosan (180 °C), was detected for the SiO_2@PMAA@SiO_2@CS nanorods. Based on the weight loss data, the weight ratio between PMAA and CS in the prepared hollow polymeric nanorods was estimated to be 2.9 : 1.0 (w/w).

The biodegradability of chitosan and PMAA has been well documented.[36–38] Because the drug release rate is associated with the degradation of materials, we measured the drug release rate from the nanorods, which showed nearly 90% of the drug could be released in 48 h (Fig. 4a).

To assess the potential of these nanorods for biomedical applications, fluorescein isothiocyanate (FITC) labeled hollow nanorods were synthesized and examined for uptake in the cell culture medium. Human lung carcinoma A-549 cell line was selected as the model. These cells were incubated with the FITC labeled nanorods for 4 h, and uptake was then imaged using a fluorescence microscope. Fig. 4b revealed a high efficiency of cellular uptake of these nanorods, suggesting their potential to function as drug carriers to achieve intracellular drug delivery.

In order to evaluate the real-time feasibility of these hollow nanorods for drug delivery in cancer therapy, docetaxel was selected as the model drug for preliminary *in vitro* cytotoxicity studies. For drug loading, the mesoporous silica nanorods were exposed to a chloroform solution containing docetaxel. After removing the silica templates, the docetaxel molecules agglomerated into clusters, thereby being retained in the hydrophobic hollow core of the polymeric nanorods.[13] The drug-loading capacity, measured by the HPLC assay, was estimated to be 12.8 wt%. For the cell cytotoxicity study, these drug-loaded nanorods were incubated with human lung carcinoma A-549 cells at different doses, followed by measuring the cell viability by the standard MTT assay. Results

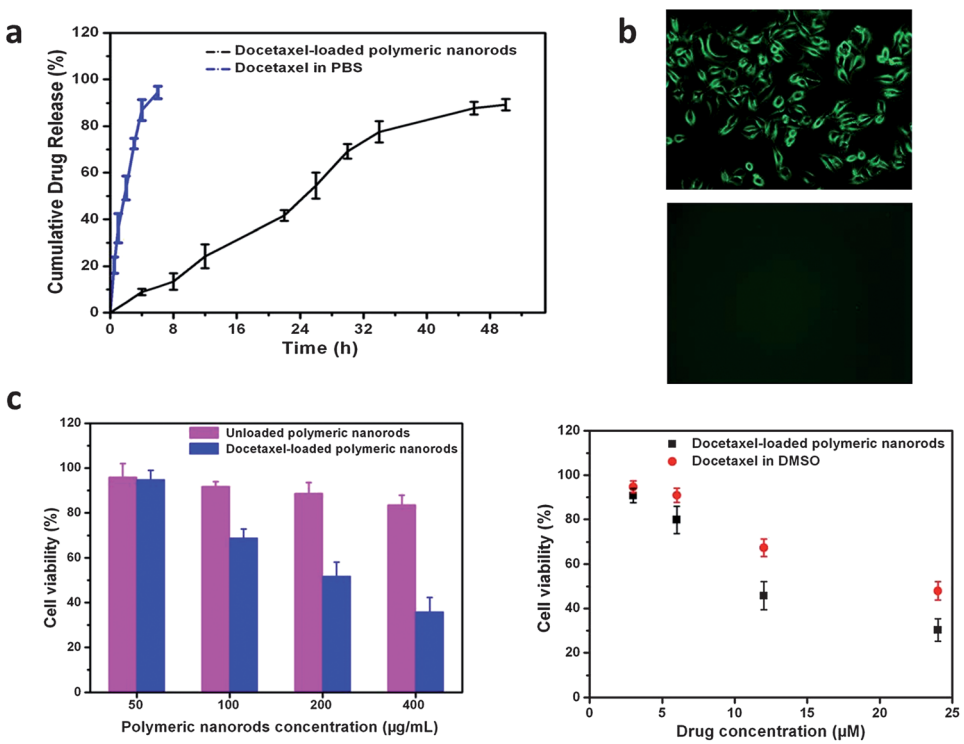

Fig. 4 (a) *In vitro* docetaxel release from docetaxel-loaded polymeric nanorods (black) and phosphate buffered solution (blue). (b) Fluorescence microscope image of A-549 cells incubated with (upper) and without (lower) FITC-labeled PMAA@CS hollow nanorods. (c) MTT assay of drug-loaded nanorods on A-549 cells. Cells were incubated with the nanorod samples for 48 h. Comparison of in cell viability between hollow polymeric nanorods without (red) and with (blue) loading of docetaxel at different doses (left), and free docetaxel and docetaxel-loaded hollow polymeric nanorods (right). Data was presented as mean ± standard deviation. Experiments were conducted in triplicate.

showed that while the blank PMAA@CS nanorods exhibited no measurable effect on cell growth (Fig. 4c), consistent with the cytotoxicity findings reported in the literature for CS,[39,40] the docetaxel-loaded nanorods yielded a markedly reduced cell viability in a dose-dependent manner (Fig. 4c). In contrast, cell cytotoxicity caused by free docetaxel in DMSO was also examined. As seen in Fig. 4c (right panel), a higher inhibition in tumor cell growth by the drug-loaded nanorods over the free drug was observed. This finding was somewhat anticipated, because with the considerable cellular uptake of the nanorod carrier displayed in Fig. 4b, a significantly elevated docetaxel concentration inside the cells would be expected compared to free docetaxel due to the relatively high level of docetaxel in the nanorod vehicles.

CS-based carriers normally bear strong cations. Due to the neutralization of anionic poly(methacrylic acid) (PMAA) with cationic CS, however, the nanorods showed a slight positive charge. In cellular studies, no precipitation of nanorods was observed, indicating their stability. Moreover, it should be mentioned that rod-shaped materials usually compare favorably to spherical materials in blood circulation longevity and tumor accumulation.[41,42]

Conclusions

Presented herein is an innovative method for synthesizing a PMAA@CS-based multilayer-hybrid hollow polymeric nanorod drug carrier by utilizing mesoporous silica nanorod templates. Uptake studies using human lung carcinoma A-549 cell lines revealed a highly efficient cell-internalization of the FITC-labeled nanorods. Cell viability studies of the docetaxel-loaded nanorods also yielded consistent results, as the drug-loaded nanorods produced a significantly higher inhibition of the growth of A-549 tumor cells when compared with treatment by free docetaxel. Given the diversity of polymerization techniques in customizing the properties of these nanorods as well as their demonstrated abilities in cell-internalization, the prospect of achieving effective intracellular delivery of anti-cancer agents by using these nanorods appears extremely promising. Further *in vivo* animal investigation of the drug-loaded nanorods is currently in progress in our laboratory.

Acknowledgements

We acknowledge the financial support of the National Basic Research Program of China (973 Program 2013CB932503), National Science Foundation of China (NNSFC 21176173), the Tianjin Municipal Natural Science Foundation (10JCYBJC14200), the State Key Laboratory of Chemical Engineering of China (SKL-CHE-11B02) and the Innovation Foundation of Tianjin University (60302068). This work was also supported in part by Grant R31-2008-000-10103-01 from the World Class University (WCU) project of the MEST and NRE of South Korea. Victor C. Yang is currently a Participating Faculty in the Department of Molecular Medicine and Biopharmaceutical Sciences, College of Medicine & College of Pharmacy, Seoul National University, South Korea.

Notes and references

1 X. Huang, I. H. El-Sayed, W. Qian and M. A. El-Sayed, *J. Am. Chem. Soc.*, 2006, **128**, 2115–2120.
2 H. Wang, T. B. Huff, D. A. Zweifel, W. He, P. S. Low, A. Wei and J. X. Cheng, *Proc. Natl. Acad. Sci. U. S. A.*, 2005, **102**, 15752–15756.
3 A. Wijaya, S. B. Schaffer, I. G. Pallares and K. Hamad-Schifferli, *ACS Nano*, 2009, **3**, 80–86.
4 B. Wildt, P. Mali and P. C. Searson, *Langmuir*, 2006, **22**, 10528–10534.
5 S. E. A. Gratton, P. A. Ropp, P. D. Pohlhaus, J. C. Luft, V. J. Madden, M. E. Napier and J. M. DeSimone, *Proc. Natl. Acad. Sci. U. S. A.*, 2008, **105**, 11613–11618.
6 F. Buyukserin and C. R. Martin, *Appl. Surf. Sci.*, 2010, **256**, 7700–7705.
7 J. L. Perry, P. Guo, S. K. Johnson, H. Mukaibo, J. D. Stewart and C. R. Martin, *Nanomedicine*, 2010, **5**, 1151–1160.
8 A. M. Alkilany, L. B. Thompson, S. P. Boulos, P. N. Sisco and C. J. Murphy, *Adv. Drug Delivery Rev.*, 2012, **64**, 190–199.
9 C. P. Tsai, Y. Hung, Y. H. Chou, D. M. Huang, J. K. Hsiao, C. Chang, Y. C. Chen and C. Y. Mou, *Small*, 2008, **4**, 186–191.
10 T. Niidome, M. Yamagata, Y. Okamoto, Y. Akiyama, H. Takahashi, T. Kawano, Y. Katayama and Y. Niidome, *J. Controlled Release*, 2006, **114**, 343–347.
11 S. Giri, B. G. Trewyn, M. P. Stellmaker and V. S. Y. Lin, *Angew. Chem., Int. Ed.*, 2005, **44**, 5038–5044.
12 M. Liong, J. Lu, M. Kovochich, T. Xia, S. G. Ruehm, A. E. Nel, F. Tamanoi and J. I. Zink, *ACS Nano*, 2008, **2**, 889–896.
13 Y. Wang, Y. Yan, J. Cui, L. Hosta-Rigau, J. K. Heath, E. C. Nice and F. Caruso, *Adv. Mater.*, 2010, **22**, 4293–4297.
14 Y. Xiao, H. Hong, V. Z. Matson, A. Javadi, W. Xu, Y. Yang, Y. Zhang, J. W. Engle, R. J. Nickles and W. Cai, *Theranostics*, 2012, **2**, 757.
15 R. Tiwari, G. Tiwari, B. Srivastava and A. K. Rai, *Int. J. PharmTech Res.*, 2009, **1**, 1338–1349.
16 S. Wang, H. Wang, W. Liang and Y. Huang, *Nanoscale Res. Lett.*, 2012, **7**, 219.
17 A. Raizada, A. Bandari and B. Kumar, *International Journal of Pharmaceutical Research and Development*, 2010, **2**, 9–20.
18 W. B. Liechty, D. R. Kryscio, B. V. Slaughter and N. A. Peppas, *Annu. Rev. Chem. Biomol. Eng.*, 2010, **1**, 149.
19 G. L. Li, C. L. Lei, C. H. Wang, K. G. Neoh, E. T. Kang and X. L. Yang, *Macromolecules*, 2008, **41**, 9487–9490.
20 P. Bawa, V. Pillay, Y. E. Choonara and L. C. du Toit, *Biomed. Mater.*, 2009, **4**, 022001.
21 Z. Qian, Z. Zhang, H. Li, H. Liu and Z. Hu, *J. Polym. Sci., Part A: Polym. Chem.*, 2008, **46**, 228–237.
22 W. Wei, L. Yuan, G. Hu, L. Y. Wang, J. Wu, X. Hu, Z. G. Su and G. H. Ma, *Adv. Mater.*, 2008, **20**, 2292–2296.
23 M. Vallet-Regí, F. Balas and D. Arcos, *Angew. Chem., Int. Ed.*, 2007, **46**, 7548–7558.
24 M. Manzano and M. Vallet-Regí, *J. Mater. Chem.*, 2010, **20**, 5593–5604.
25 J. L. Vivero-Escoto, I. I. Slowing, B. G. Trewyn and V. S. Y. Lin, *Small*, 2010, **6**, 1952–1967.

26 S. P. Hudson, R. F. Padera, R. Langer and D. S. Kohane, *Biomaterials*, 2008, **29**, 4045–4055.
27 S. J. Clarke and L. P. Rivory, *Clin. Pharmacokinet.*, 1999, **36**, 99–114.
28 K. A. Lyseng-Williamson and C. Fenton, *Drugs*, 2005, **65**, 2513–2531.
29 X. L. Huang, X. Teng, D. Chen, F. Q. Tang and J. Q. He, *Biomaterials*, 2010, **31**, 438–448.
30 W. Stöber, A. Fink and E. Bohn, *J. Colloid Interface Sci.*, 1968, **26**, 62–69.
31 E. Bourgeat-Lami and J. Lang, *J. Colloid Interface Sci.*, 1998, **197**, 293–308.
32 G. Li, G. Liu, E. T. Kang, K. G. Neoh and X. Yang, *Langmuir*, 2008, **24**, 9050–9055.
33 A. P. Leonov, J. W. Zheng, J. D. Clogston, S. T. Stern, A. K. Patri and A. Wei, *ACS Nano*, 2008, **2**, 2481–2488.
34 W. Xia, H.-M. Song, Q. Wei and A. Wei, *Nanoscale*, 2012, **4**, 7143–7148.
35 Y. J. Zhang, Y. Guan and S. Q. Zhou, *Biomacromolecules*, 2005, **6**, 2365–2369.
36 M. Amidi, E. Mastrobattista, W. Jiskoot and W. E. Hennink, *Adv. Drug Delivery Rev.*, 2010, **62**, 59–82.
37 S. Sajeesh, K. Bouchemal, C. Sharma and C. Vauthier, *Eur. J. Pharm. Biopharm.*, 2010, **74**, 209–218.
38 H. Pawar, D. Douroumis and J. S. Boateng, *Colloids Surf., B*, 2012, **90**, 102–108.
39 M. Garcia-Fuentes, C. Prego, D. Torres and M. J. Alonso, *Eur. J. Pharm. Sci.*, 2005, **25**, 133–143.
40 M. V. Lozano, D. Torrecilla, D. Torres, A. Vidal, F. Dominguez and M. J. Alonso, *Biomacromolecules*, 2008, **9**, 2186–2193.
41 Y. Geng, P. Dalhaimer, S. Cai, R. Tsai, M. Tewari, T. Minko and D. E. Discher, *Nat. Nanotechnol.*, 2007, **2**, 249–255.
42 A. Albanese, P. S. Tang and W. C. W. Chan, *Annu. Rev. Biomed. Eng.*, 2012, **14**, 1–16.